Structural Investigations of Vapochromic Behavior. X-ray Single-Crystal and Powder Diffraction Studies of $[Pt(CN\text{-}iso\text{-}C_3H_7)_4][M(CN)_4]$ for M = Pt or Pd

Carrie E. Buss, Carolyn E. Anderson, Marie K. Pomije, Christopher M. Lutz, Doyle Britton, and Kent R. Mann*

Contribution from the Department of Chemistry University of Minnesota, Minneapolis, Minnesota 55455-0431

Received April 10, 1998

Abstract: We have synthesized $[Pt(CN\text{-}iso\text{-}C_3H_7)_4][M(CN)_4]$ (M = Pt, Pd) and studied their reversible hydration and sorption properties with UV−vis, FT-IR spectroscopy, and X-ray diffraction. Powder diffraction studies show that anhydrous $[Pt(CN\text{-}iso\text{-}C_3H_7)_4][Pt(CN)_4]$ and $[Pt(CN\text{-}iso\text{-}C_3H_7)_4][Pd(CN)_4]$ crystallize in a tetragonal space group with nearly identical lattice constants. Gravimetric studies reveal that variable guest−host stoichiometries occur when solid $[Pt(CN\text{-}iso\text{-}C_3H_7)_4][Pt(CN)_4]$ sorbs the guest at room temperature from the gas phase [water, 12.1(1) molecules per formula unit, chloroform 6.0(1), methanol 8.0(1), and trifluoroethanol 4.1(1)]; these sorption processes are reversible. The unit cell distances in the tetragonal *ab*-plane expand dramatically when the solvent guests are sorbed, but changes along the *c*-axis (the M−M direction) are minimal. Crystallization of $[Pt(CN\text{-}iso\text{-}C_3H_7)_4][Pt(CN)_4]$ from water gives monoclinic crystals of a hexadecahydrate $[Pt(CN\text{-}iso\text{-}C_3H_7)_4][Pt(CN)_4]\cdot 16H_2O$. This salt consists of alternating cation/anion chains along *b* with an average Pt−Pt distance of $b/2 = 3.1521(1)$ Å. The sixteen water molecules per formula weight interlace neighboring chains via H-bonding with each other and the CN^- ions of the $Pt(CN)_4^{2-}$ units. The shifts in the UV−vis and IR spectra that occur when solvent guests are sorbed by the double complex salts are discussed in terms of the lattice expansions that are observed. A mechanism for the lattice expansions that accompany the sorption of guest molecules is proposed.

Introduction

We have reported studies with square-planar d^8 platinum complexes that could be used as the chemically sensitive layer for a chemical sensor system.[1] These complexes are robust and form intensely colored solid-state materials that respond spectroscopically to a wide range of volatile organic compounds (VOCs); this process has been named vapochromism.[2] More recently, we have studied the vapochromic shifts that occur in the solid-state UV−vis, NIR, and IR spectra of $[Pt(p\text{-}CN\text{-}C_6H_4\text{-}C_{10}H_{21})_4][M(CN)_4]$ (M = Pd, Pt).[3] These studies suggest that sorbed guest molecules capable of significant H-bonding interact with the cyanide ligands to produce shifts in the ν(CN) stretching frequencies that also correlate with the UV−vis changes.

A more detailed analysis of the vapochromic effect in these platinum complexes has been hampered by the lack of crystallographic data to correlate structural changes with the observed vapochromic shifts. Herein, we report the synthesis and X-ray powder diffraction studies of a series of hydrated and solvated $[Pt(CN\text{-}iso\text{-}C_3H_7)_4][M(CN)_4]$ (M = Pt, Pd) complexes (abbreviated **PtPt** and **PtPd**, respectively). The powder diffraction data are correlated with a single-crystal diffraction study of a monoclinic hexadecahydrate, **PtPt**·$16H_2O$. These studies show that vapochromism in the **PtPt** and **PtPd** systems is accompanied by large reversible increases in the unit cell dimensions perpendicular to the M−M direction. The large (50−90%) unit cell increases allow the reversible inclusion of solvent molecules.

Experimental Section

General Considerations. Isopropylisocyanide was purchased from the Strem Chemical Company. Elemental analyses were performed by MHW Laboratories or QTI Analytical Laboratories. $Pt(CH_3CN)_2Cl_2$ was prepared from $K_2[PtCl_4]$ as previously reported.[4] $[(n\text{-}C_4H_9)_4N]_2[M(CN)_4]$ (M = Pt, Pd) were prepared from $[(n\text{-}C_4H_9)_4N]Br$ (Aldrich) and $K_2[M(CN)_4]$ (Strem) as previously reported.[5] All solvents used in the IR studies were ACS Reagent grade and used as received after drying over molecular sieves.

UV−vis absorption spectra were recorded on a previously described Tracor Northern TN-6500 rapid-scan diode-array spectrometer[6] equipped with a xenon-arc source. Sample films of double-complex salts were spin-coated from methanol solution onto 1.0 × 2.5 cm microscope slides. A coated slide was held flat against the inside wall of a four-sided quartz cell by a copper spring.

Infrared absorption spectra were obtained with use of the attenuated total reflectance (ATR) method on a Nicolet Magna-IR System 550 spectrometer equipped with a ZnSe trough HATR cell from PIKE Technologies. Data were processed with OMNIC ESP v. 4.1 software. Sample films were coated on the ZnSe crystal from an ether suspension or methanol solution. For vapochromic experiments, a beaker filled with glass wool saturated with several milliliters of VOC was placed

* To whom correspondence should be addressed.

(1) (a) Exstrom, C. L.; Sowa, J. R.; Daws, C. A.; Janzen, D. E.; Mann, K. R. *Chem. Mater.* **1995**, *7*, 15. (b) Daws, C. A.; Exstrom, C. L.; Sowa, J. R.; Mann, K. R. *Chem. Mater.* **1997**, 9, 363.

(2) Nagel, C. C. U. S. Patent 4,834,909, 1989.

(3) Exstrom, C. L.; Pomije, M. K.; Mann, K. R. *Chem. Mater.* **1998**, *10*, 942.

(4) Fanizzi, F. P.; Intini, L.; Maresca, L.; Natile, G. *J. Chem. Soc., Dalton Trans.* **1990**, 199.

(5) Mason, W. R.; Gray, H. B. *J. Am. Chem. Soc.* **1968,** *90*, 5721.

(6) Bullock, J. P.; Mann, K. R. *Inorg. Chem.* **1989**, *28*, 4006.

S0002-7863(98)01218-9 CCC: $15.00
Published on Web 07/17/1998

on the ZnSe mount and the ATR cell was then rapidly covered. Spectra were recorded as the equilibrium vapor pressure of the VOC was established and after the VOC source was removed.

Solvent uptake/release studies were conducted by thermal gravimetric analysis TGA (Perkin-Elmer TGA 7 instrument) or by gravimetric analysis (Mettler AE50 electronic balance). Guest saturated TGA samples were prepared by allowing the double-complex salt to equilibrate with the VOC vapor/liquid overnight. A 7−10 mg sample was quickly transferred to the platinum pan and the sample compartment was purged with nitrogen gas for 1 h to remove all traces of residual water (typically 1−2 equiv) prior to heating. The balance experiments were conducted in a 100 mL three-necked flask fitted with stopcocks and a 10 cm ground glass tube on the center neck. A stainless steel wire was hung from the hook arm underneath the balance and attached to a holder designed for a 1 cm diameter aluminum pan. Samples (35 to 50 mg) were placed in the pan, set on the holder, and suspended down the tube into the flask. After nitrogen was purged through the apparatus until a constant mass was obtained, 1 to 2 mL of liquid VOC was added by syringe to the bottom of the flask. Sample mass was recorded as a function of time. After a constant mass was obtained, the remaining liquid VOC was removed by syringe and the chamber purged with nitrogen until constant mass was again obtained.

[Pt(CN-*iso*-C_3H_7)$_4$][Pt(CN)$_4$] (PtPt). The procedure for the previously prepared compound [Pt(*p*-CN-C_6H_4-$C_{10}H_{21}$)$_4$][Pt(CN)$_4$][1] was followed with $Pt(CH_3CN)_2Cl_2$ (0.45 g, 1.31 mmol), [(*n*-Bu)$_4$N]$_2$[Pt(CN)$_4$] (1.04 g, 1.33 mmol, 1.0 equiv), isopropylisocyanide (0.57 mL, 6.27 mmol, 5.07 equiv) and acetonitrile (30 mL). Stirring for 4 h yielded a red-violet precipitate with a distinctive green metallic shine (yield = 0.76 g, 76%). IR ν(C≡NR) = 2274 cm^{-1} (vs), ν(C≡N) = 2127 cm^{-1} (vs). UV−vis (spin-coated film on microscope slide): λ_{max} = 593 nm. Anal. Calcd (partially hydrated formula **PtPt**·2.24H_2O): C, 29.85; H, 4.036; N, 13.82. Found: C, 29.85; H, 3.32; N, 13.71.

[Pt(CN-*iso*-C_3H_7)$_4$][Pd(CN)$_4$] (PtPd). The procedure followed that above for Pt(CN-*iso*-C_3H_7)$_4$][Pd(CN)$_4$] with $Pt(CH_3CN)_2Cl_2$ (0.51 g, 1.48 mmol), [(n-Bu)$_4$N]$_2$[Pd(CN)$_4$] (1.63 g, 1.49 mmol, 1.01 equiv), isopropylisocyanide (0.63 mL, 6.92 mmol, 4.69 equiv) and acetonitrile (40 mL). Upon addition of isopropylisocyanide a lemon yellow solid precipitated. After the mixture was stirred for 2 h, 0.54 g of the product was isolated (53% yield). IR: ν(C≡NR) = 2275 cm^{-1} (vs), ν(C≡N) = 2127 cm^{-1} (vs). UV−vis (film spin coated on microscope slide): λ_{max} = 437 nm. Anal. Calcd (partially hydrated formula **PtPd**·0.4H_2O): C, 34.86; H, 4.21; N, 16.26. Found: C, 34.86; H, 3.94; N, 16.26.

X-ray Powder Diffraction Patterns. X-ray Powder Diffraction Patterns were collected at room temperature (22 °C) with Siemens D-500 or D-5005 diffractometers with a 2.2 kW sealed copper source equipped with a single-crystal graphite monochromator and scintillation counter. Data were processed with use of Jade V 3.0 software. Complete powder diffraction patterns ("long" scans, 1 h 40 min) were collected for 2θ = 2−60° with slits = [1°, 1°, 1°, 0.15°, 0.15°], 2θ stepping rate = 0.02°, and angle dwelling rate = 2 s.

The sample cell was constructed by glueing four glass microscope slide covers to a 45 mm × 45 mm × 3.2 mm glass plate. The slide covers were arranged to produce a 7.8 mm × 23.3 mm indentation 0.4 mm deep. This arrangement forms a thin sample well that requires a small sample size (≈20 mg) and allows rapid equibration of the solid with solvent vapor.

The samples were thoroughly dried under vacuum overnight and transferred under dry nitrogen into the sample holder. The powder samples were not ground before packing in the sample holder because shear pressure partially isomerizes the double salts into the neutral form.[7] Typically, the powders were packed into the sample well and leveled off with a microscope slide, using as little direct pressure as possible.

X-ray vapochromic experiments were carried out by enclosing the sample holder in a small resealable plastic bag. A dry atmosphere was maintained in the bag (when required) by the presence of fresh P_2O_5. Subsequent data analysis revealed that this procedure was adequate to maintain the **PtPt** and **PtPd** systems in the anhydrous state. The powder patterns collected for samples enclosed in the bag show a slight increase in the intensity of the baseline, but do not contain additional reflections in the 2θ = 2−60° data collection range. The bag enclosure around the sample cell allows exposure of the sample to VOCs without disturbing the packing of the powder in the sample well. The samples were exposed to VOCs by placing glass wool saturated with 5−6 mL of VOC in the bag that was then sealed to create a room-temperature atmosphere saturated with the VOC vapors. The sample, vapor, and liquid VOC were allowed to come to equilibrium. The equilibration period was monitored by collecting fast "snapshot" scans until the position of the reflections became constant. These "snapshot" scans (∼10 min) were typically collected for 2θ = 2−40° or 2−20° with slits = [1°, 1°, 1°, 0.15°, 0.15°] or [1°, 1°, 1°, 0.6°, 0.6°], 2θ stepping rate = 0.05°, and angle dwell = 1 s. Once the peak positions were stable a long scan was collected. The remaining liquid VOC was then removed from the bag and the sample was allowed to equilibrate in air, using snapshot scans to monitor the reversibility of the VOC exposure. When the positions of the reflections again became constant a long scan was collected.

Table 1. Crystal Data, Data Collection, and Refinement Parameters for PtPt·16H_2O

formula	$C_{20}H_{60}N_8O_{16}Pt_2$	V, Å^3	4376.1(1)
habit, color	needle, red	Z	4
size, mm	0.50 × 0.20 × 0.15	fwt, g mol^{-1}	1058.9
lattice type	monoclinic	D_c, g cm^{-3}	1.607
space group	*C*2/*c*	μ, mm^{-1}	6.448
a, Å	32.2966(4)	*F*(000)	2080
b, Å	6.3042(1)	λ, Å	0.71073
c, Å	24.7833(3)	*T*, K	173(2)
β, deg	119.859(1)		

diffractometer	Siemens SMART Platform CCD
θ range, deg	1.45 to 25.17
index ranges	$-38 \le h \le 33$, $0 \le k \le 7$, $0 \le l \le 29$
no. of reflcns collected	17965
no. of unique reflcns	3827 (R_{int} = 0.021)
system used	SHELXTL-V5.0
solution	direct methods
refinement method	full-matrix least-squares on F^2
weighting factors,[a] *a*, *b*	0.039, 2.855
absorption correction	SADABS
max, min transmission	1.000, 0.736
extinction coeff	0.00021(3)
no. of data, restraints, parameters	3824, 0, 216
R_1, wR_2 ($I > 2\,\sigma(I)$ = 2794)	0.026, 0.069
R_1, wR_2 (all data)	0.038, 0.079
goodness-of-fit (on F^2)	1.062
largest diff peak, hole, e Å^{-3}	1.70, −1.27

[a] $w^{-1} = [\sigma^2(F_o^2) + (aP)^2 + (bP)]$, where $P = (F_o^2 + 2F_c^2)/3$.

Collection and Reduction of Crystallographic Data for the Single-Crystal Diffraction Study of PtPt·16H_2O. A solution of **PtPt** in water was filtered and then left open to the laboratory atmosphere. Bright red, needlelike crystals of **PtPt**·16H_2O formed overnight. A crystal measuring approximately 0.50 × 0.20 × 0.15 mm was attached to a glass fiber and mounted on the Siemens SMART system[8] for data collection at 173(2) K. Crystal and X-ray collection and refinement data are summarized in Table 1.

The space group *C*2/*c* was determined on the basis of systematic absences and intensity statistics. A direct-methods solution[8] provided the positions of most non-hydrogen atoms. Several full-matrix least-squares/difference Fourier cycles were performed to locate the remaining non-hydrogen atoms. The anisotropic displacement parameters for the carbon atoms in the isopropyl group attached to N3 indicate disorder in this group. Attempts to refine the disorder with use of two partially occupied sets of positions did not lead to any improvement in wR_2 nor to better bond lengths and angles. For the final refinement this was left as abnormal anisotropy. All non-hydrogen atoms were refined with

(7) Grinding the double salt compounds causes solid-state reactions that isomerize the $Pt(CNR)_4M(CN)_4$ to the neutral $M(CNR)_2(CN)_2$ compounds.

(8) Siemens SMART Platform CCD, Siemens Industrial Automation, Inc.: Madison, WI.

Table 2. Selected Interatomic Distances (Å)[a] and Angles (deg)[a] for **PtPt**·$16H_2O$

Pt(1)−Pt(2)	3.1617(3)	Pt(1)−Pt(2)[b]	3.1425(3)
Pt(1)−C(1)	1.989(5)	Pt(1)−C(2)	1.987(5)
Pt(2)−C(3)	1.971(5)	Pt(2)−C(4)	1.974(5)
C(1)−N(1)	1.140(6)	C(2)−N(2)	1.145(6)
C(3)−N(3)	1.128(6)	C(4)−N(4)	1.132(6)
N(3)−C(31)	1.459(7)	N(4)−C(41)	1.457(7)
C(31)−C(32)	1.335(9)	C(41)−C(42)	1.503(7)
C(31)−C(33)	1.389(8)	C(41)−C(43)	1.512(8)
C(1)−Pt(1)−C(1)[c]	179.4(2)	C(2)−Pt(1)−C(2)[c]	179.2(2)
C(3)−Pt(2)−C(3)[c]	178.2(2)	C(4)−Pt(2)−C(4)[c]	179.6(2)
C(1)−Pt(1)−Pt(2)	90.29(12)	C(3)−Pt(2)−C(4)	88.2(2)

[a] Estimated standard deviations in the least significant figure are given in parentheses. [b] x, $1 + y$, z. [c] $-x$, y, $1/2 - z$.

anisotropic displacement parameters. Hydrogen atoms on the ligands were placed in idealized positions and refined as riding atoms with isotropic displacement parameters 20% larger than the equivalent isotropic displacement parameter of the attached atom. Only six of the sixteen possible hydrogen atoms on the water molecules could be located with moderate certainty. The remaining 10 could not be located and have not been included in the refinement.

The asymmetric unit is one-half of the formula unit of the complex along with eight water molecules. Both platinum atoms were located on the crystallographic 2-fold axis. The two largest peaks in the difference Fourier map with heights greater than 1 e/Å^3 are near respective platinum atoms: height 1.70 e/Å^3, 0.94 Å from Pt1; height 1.65 e/Å^3, 0.95 Å from Pt2. All calculations were performed with the SHELXTL V5.0 suite of programs.[9] Table 2, sections a and b, contains selected distances and angles. Complete tables of positional parameters and least-squares planes are given in the Supporting Information.

Results

Synthesis and Characterization. Samples of **PtPt**·$x H_2O$ and **PtPd**·$x H_2O$ with variable degrees of hydration are readily synthesized by a modification[1] of the method of Nagle.[2] Stirring a solution containing $Pt(CH_3CN)_2Cl_2$, $[(n\text{-}Bu)_4N]_2[M(CN)_4]$, and isopropylisocyanide in acetonitrile affords microcrystalline precipitates of the desired compounds in 76% and 53% yields, respectively. Elemental analyses were obtained for samples of both compounds that retained small amounts of water (as determined by TGA). These partially hydrated samples were convenient to handle in laboratory air and were easily dried to the anhydrous state (see Experimental Section) as needed for further experiments. The ease that these materials undergo hydration/dehydration cycles is consistent with their sorption properties (vide infra). As previously observed for similar compounds,[1b] solid **PtPt** is much more stable than the **PtPd** analogue. Exposure of **PtPd** to 100% relative humidity air resulted in significant decomposition after 1 day; in contrast, **PtPt** is stable under identical conditions for at least a week. Bulk samples of **PtPt** are red with a green metallic reflectance while **PtPd** is bright lemon yellow. Microscopic examination of partially hydrated **PtPt** shows the bulk material consists of thin red-violet hair-like crystals that have an intense green reflection at certain angles. Microscope slides coated with the compounds used for vapochromic studies are violet and yellow, respectively.

UV−vis Vapochromic Studies. An investigation of the solid-state UV−vis spectra of the two compounds in the dry state shows that **PtPt** has a broad intense band at 593 nm and a weak peak at 333 nm, while **PtPd** has a single band at 437 nm. The lowest energy band is intimately associated with the M−M interaction as previously discussed.[1,10] The vapochromic shifts of this band for **PtPt** are reported in Table 3. The low-energy band blue shifts in response to methanol, water, and trifluoroethanol vapors, while exposure to chloroform vapor results in a red shift. As discussed previously for the $[Pt(p\text{-}CN\text{-}C_6H_4\text{-}C_{10}H_{21})_4][Pt(CN)_4]$ system,[3] the correlation between VOC character and the UV−vis vapochromic shift is complicated and not completely understood.

Infrared Vapochromic Experiments. Information concerning the interactions between the VOC guest and the **PtPt** host has been obtained with ATR FTIR spectroscopy in the C≡N stretching region (2100−2300 cm^{-1}) of the mid-IR. A well-formed dry film of **PtPt** deposited on the ATR crystal appears green and metallic. This film shows a strong vibration at $\nu_{CN} = 2127$ cm^{-1} due to the ligands of the $[Pt(CN)_4]^{2-}$ anion and an isocyanide stretch $\nu_{CNR} = 2274$ cm^{-1} due to the $[Pt(CN\text{-}C_3)_4]^{2+}$ cation. The cyanide stretch is sensitive to the presence of VOCs in the host lattice.[1,3] The ν_{CN} peak positions during exposure of films of **PtPt** to methanol, water, trifluoroethanol and chloroform vapors are presented in Table 3. The ν_{CN} peak shift correlates with the hydrogen bonding ability of the VOC in a manner consistent with the more extensively studied $[Pt(p\text{-}CN\text{-}C_6H_4\text{-}C_{10}H_{21})_4][Pt(CN)_4]$ system.[1,3]

Single-Crystal Structure of PtPt·$16H_2O$. Single-crystal data for **PtPt**·$16H_2O$ are in Table 1; selected bond lengths and angles are in Table 2. The structure of **PtPt**·$16H_2O$ contains infinite stacks of alternating square-planar cations and anions (Figures 1 and 2) along the *b*-axis with Pt−Pt separations that average to $b/2 = 3.1521(3)$ Å. The unit cell symmetry allows two alternating inter-platinum distances (3.1425(3) and 3.1617(3) Å) along the chains so that the solid formally contains stacks of ion pairs. Alternating cation−anion stacking is reminiscent of a model compound, Magnus' Green Salt[11] (MGS, $[Pt(NH_3)_4][Pt(Cl)_4]$; $c = 6.49$ Å, Pt−Pt = 3.245 Å)[12] and a more recently reported compound $[Pt(CNCH_3)_4][Pd(mnt)_2]$[13] (mnt = thiomaleonitrile; $b = 6.614(1)$ Å, Pt−Pd = 3.307(1) Å). A significant difference between MGS and **PtPt**·$16H_2O$ lies in the arrangement of the chains relative to each other. The four chains at the corners of the tetragonal cell in MGS are displaced 1/2 the unit cell length along *c* to yield pseudocentering of the Pt atoms in the cations and anions in the tetragonal *ab* plane. The chain arrangement in **PtPt**·$16H_2O$ is such that the two chains in the monoclinic unit cell are displaced ∼3/10 the unit cell length along *b* relative to one another. This arrangement results in "slippage" of the adjacent chains so that the cations are not coplanar with the closest neighbor anions.

The $M(CN)_4$ fragments of both the cation and the anion have only 2-fold symmetry required crystallographically, but actually are very close to the expected D_{4h}, as can be seen from data in Table 2. The cation and anion are almost perfectly staggered (mean torsion angle 39.8°), presumably to minimize the steric repulsion of the ligands above and below each square plane and to optimize the close approach of the metal centers. In MGS this torsion angle is 28°. Both Pt−C−N−C fragments in the cation are close to linear but the isopropyl groups are rotated differently with respect to the $M(CN)_4$ plane (torsion angles: Pt(1)−Pt(2)···C(31)−H(31), −119°; Pt(1)−Pt(2)···C(41)−H(41), −39°).

(9) Sheldrick, G. M. 1994 SHELXTL. Version 5.0, Siemens SMART Platform CCD.

(10) (a) Gliemann, G.; Yersin, H. *Struct. Bonding* **1985**, *62*, 87. (b) Miskowski, V. M.; Houlding, V. H. *Inorg. Chem.* **1991**, *30*, 4446.

(11) Magnus, G. *Pogg. Ann.* **1828**, *11*, 242.

(12) Atoji, M.; Richardson, J. W.; Rundle, R. E. *J. Am. Chem. Soc.* **1957**, *79*, 3017.

(13) Connelly, N. G.; Crossley, J. G.; Orpen, A. G.; Salter, H. *J. Chem. Soc., Chem. Commun.* **1992**, 1564.

Table 3. Unit Cell, UV−vis and IR Data for **PtM·x** Guest[a] Compounds (**M = Pt**, **Pd**)

stoichiometry	*a* (Å) *b* (Å)	*c* (Å)	unit cell *V* (Å^3)	mol vol (Å^3)[b]	packing coeff[c] C_K	UV−vis[e] λ_{max} (nm)	IR[e] ν(CN$^-$) (cm^{-1})
PtPt	14.731(1)	6.3369(9)	1375.0(1)	427	0.622	593	2127
PtPt·12H_2O	18.271(4)	6.325(1)	2111.6(7)	695	0.658	573	2137
PtPt·8MeOH	18.698(5)	6.337(2)	2215.4(9)	720	0.650	574	2139
PtPt·4CF_3CH_2OH	19.330(1)	6.362(1)	2377.1(2)	709	0.597	576	2143
PtPt·6$CHCl_3$	20.563(4)	6.303(2)	2665.3(8)	876	0.657	603	2131
PtPd	14.730(1)	6.3465(1)	1377.0(2)	427	0.620	437	2127
PtPd·12H_2O	18.224(3)	6.326(1)	2100.9(6)	695	0.661		
PtPd·8MeOH	18.679(3)	6.341(1)	2212.4(4)	720	0.651		
PtPd·4CF_3CH_2OH	19.309(4)	6.378(1)	2377.8(7)	709	0.597		
PtPd·6$CHCl_3$	20.576(5)	6.315(2)	2673.6(10)	876	0.655		
PtPt·16H_2O[d]	32.2966(4) 24.7833(3)	6.3042(1)	4376.1(1)	784	0.717		

[a] All unit cells are tetragonal with $Z = 2$ except where noted; estimated standard deviations in the least significant figure are given in parentheses. [b] Molecular volumes used in these calculations: $[Pt(CN\text{-}iso\text{-}propyl)_4]^{2+}$, 294.6 Å^3; $[Pt(CN)_4]^{2-}$, 132.8 Å^3; $[Pd(CN)_4]^{2-}$, 132.6 Å^3; H_2O, 22.3 Å^3; CH_3OH, 36.6 Å^3; CF_3CH_2OH, 70.5 Å^3; $HCCl_3$, 70.5 Å^3. [c] Kitaigorodsky packing coefficients are calculated from Z*(mol vol)/V. [d] Taken from the single-crystal data reported herein and transformed to the first setting with $\gamma = 119.859(1)°$ and $Z = 4$. [e] See Experimental Section for sampling details.

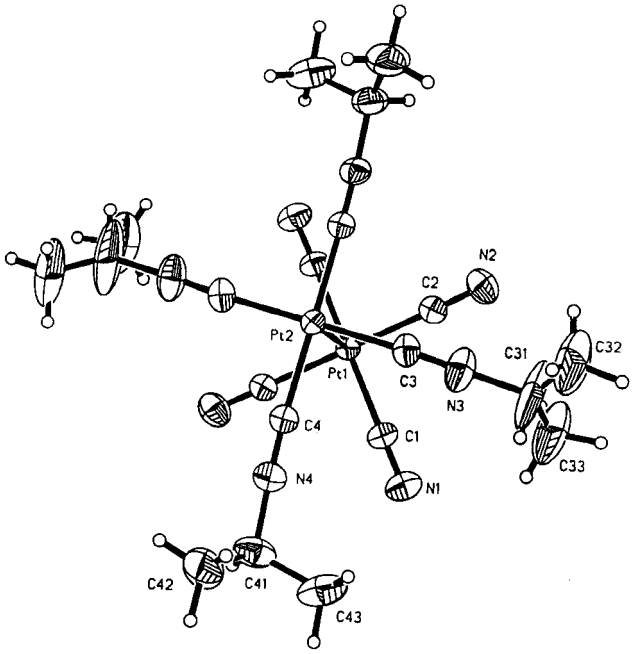

Figure 1. ORTEP diagram of the cation−anion pair in **PtPt**·16H_2O. Ellipsoids are drawn at the 50% level.

The structure also contains 16 water molecules per formula unit that separate but interconnect neighboring stacks via hydrogen bonds. Eight of these are crystallographically independent. Sixteen N···O or O···O distances are about 2.8 Å. We regard these as evidence of the 16 hydrogen bonds that might be expected to form. Three of the oxygen atoms are involved in three H-bonds and the remaining five in four. Additional H-bonds are formed to each of the CN^- ligands on the $[Pt(CN)_4]^{2-}$ anions (Figure 2); N1 is involved in one H-bond; N2 is involved in two. The connectivity of the hydrogen bonding pattern is such that most of the hydrogen positions could be disordered. The net result is hydrogen bonded regions of water molecules at approximately $x = {}^1/_4$ and $x = {}^3/_4$ in the cell. The distances and angles for the H-bonding are given in the Supporting Information.

TGA and Gravimetric Studies. TGA studies with thoroughly dried **PtPt** and **PtPd** showed that as these samples are heated, no additional mass losses are recorded up to 150 °C. Similar studies with the hydrated tetragonal forms (vide infra) showed that all twelve waters of hydration are lost when the sample compartment is purged with dry nitrogen at room temperature. Gravimetric uptake studies indicate that dry **PtPt** readily sorbs solvent molecules from the gas phase in stoichiometrically precise amounts: 12.1(1) molecules of water, 8.0(1) molecules of methanol, 6.0(1) molecules of chloroform, and 4.1(1) molecules of trifluoroethanol per formula unit, respectively. In each case the sorption is reversible and can be repeated at least several times. As the continuous exposure of **PtPt** to these solvents does not cause noticeable decomposition after many days, it is apparent that a high degree of reversibility is maintained. The sorption of these solvent vapors to completion is generally rapid (60 min) for bulk samples and much faster (seconds) for thin films.

Among the sorption data for organic solvents, methanol gave particularly interesting results (Figure 3). During the first 15 min of exposure to methanol a nearly linear gain in sample mass was observed corresponding to the sorption of 4 molecules of methanol per formula unit; from 15 to 35 min, the sample continued to gain mass linearly but at a slower rate; after 35 min the response slowed until a total of 8 molecules of methanol per formula unit were sorbed after 40 min. These results suggest that two distinct solvated phases containing 4 and 8 molecules of methanol are formed in this system. This result was confirmed by powder diffraction studies as described below.

X-ray Powder Diffraction Data for PtM·X Guest (M = Pt, Pd). In addition to the single crystal study of **PtPt**·16H_2O, X-ray powder diffraction patterns were collected for the dry, hydrated, and solvated forms of **PtPt** and **PtPd**. Single crystals were unavailable for these latter materials. These results are summarized in Table 3. In all the cases we report here, the reversible uptake of the guest solvent molecules in the gravimetric studies is accompanied by a reversible expansion of the unit cell that retains tetragonal symmetry. The expansions are quite large, but are consistent with the gravimetrically determined stoichiometries.

Data for dry **PtPt** and **PtPd** were indexed to nearly identical tetragonal unit cells with $Z = 2$ and dimensions $a = 14.731(1)$ Å and $c = 6.3369(9)$ Å for **Pt Pt** and $a = 14.730(1)$ Å and $c = 6.3465(1)$ Å for **PtPd**. Figure 4 compares these two patterns. Normally, the unambiguous placements of even the heavy atoms in a unit cell are difficult based on powder diffraction data such as those collected here. The further interpretation of these data is possible because of the close analogy to the MGS tetragonal structures.[12,14]

(14) Cradwick, M. E.; Hall, D.; Philiips, R. K. *Acta Crystallogr*. **1971**, *B27*, 480.

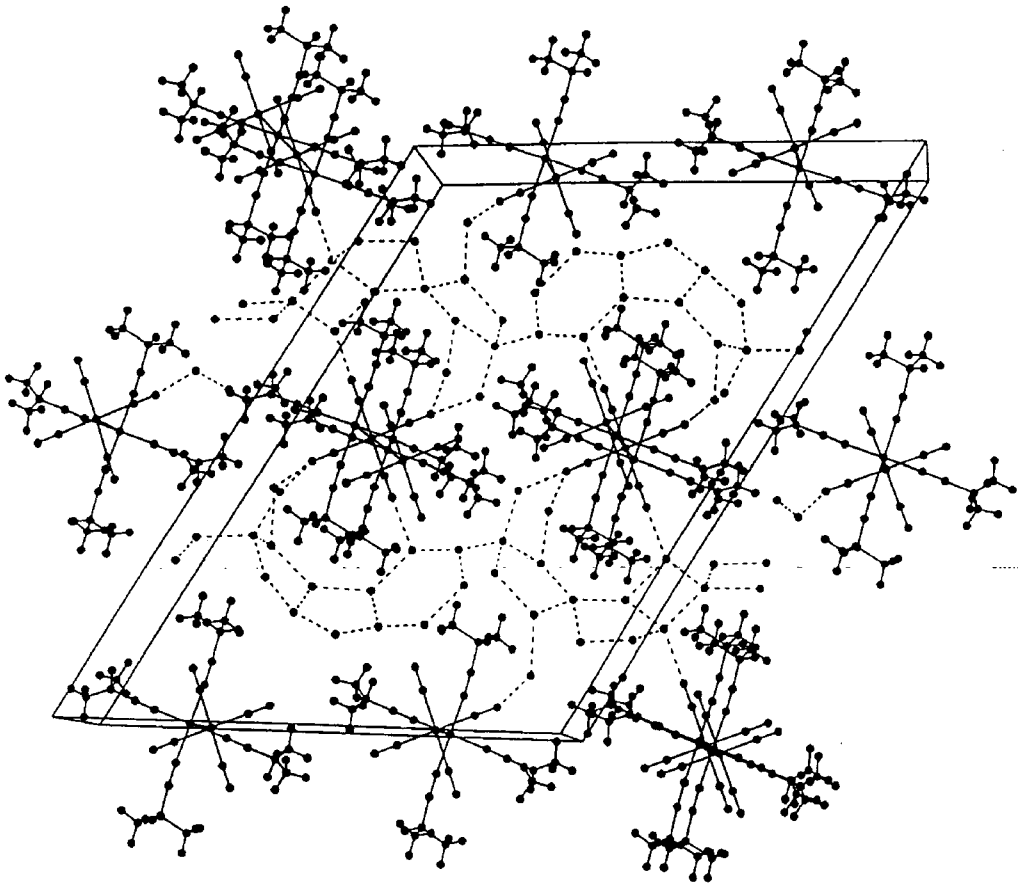

Figure 2. Solid-state packing diagram of **PtPt**·16H_2O. View down the *b*-axis; dashed lines indicate significant H-bonding interactions.

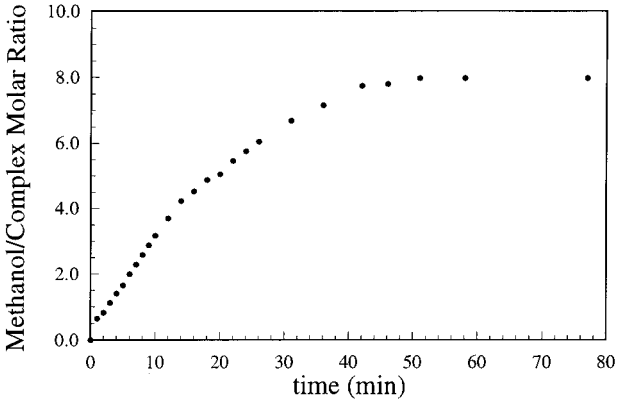

Figure 3. Gravimetric sorption of methanol vapor by **PtPt** followed as a function of time.

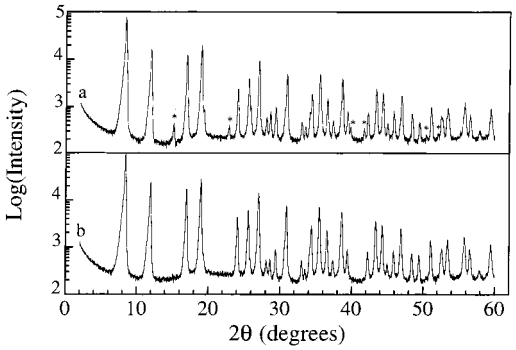

Figure 4. X-ray powder diffraction patterns of (a), **PtPd** and (b) **PtPt**. The vertical axis in each case is the log (intensity) to more clearly show the weak diffraction peaks. Peaks labeled with * are $h + k =$ odd and $l =$ odd reflections that are weak in the **PtPt** case.

X-ray diffraction from MGS is dominated by platinum scattering. The space group is *P*4/*mnc* with one ion centered at 0,0,0 and the other at 0,0,$^1/_2$. In this case, the platinum atoms contribute to the scattering only when two conditions are met: $h + k$ even, and l even. Accordingly, only reflections that meet both these conditions have high intensities. The replacement of the Pt in the anion by Pd causes a change in these conditions, i.e., the metal atoms contribute only to the $h + k + l$ even reflections. All 10 of the tetragonal structures listed in Table 4 are consistent with the appropriate set of conditions. The additional intensity observed for reflections such as 101, 301, 231, and others in the **PtPd** compounds (labeled with an asterisk in Figure 4 for the "dry" **PtPd** compound) allows the indexing of these lines and allows the *c*-axis length to be determined unambiguously. Powder diffraction patterns calculated[15] in the *P*4/*mnc* space group with $a = b = 14.72$ Å and $c = 6.33$ Å and the two metal atoms at 0,0,0 and 0,0,$^1/_2$ show these expected intensity changes and are in qualitative agreement with the experimentally determined patterns for both **PtPt** and **PtPd** when the effects of preferential orientation of the powdered samples are taken into account. These results in combination with the **PtPt**·16H_2O single-crystal results allow us to be confident in the placement of the metal atoms in the tetragonal forms of **PtPt** and **PtPd. We conclude that the heavy atom arrangement for all 10 tetragonal compounds is the same as in MGS but the $a = b$ distance is variable to accommodate the larger ligands and the guest molecules**.

Assigning these 10 structures unambiguously to the *P*4/*mnc* space group is problematic because the light atom positions

(15) (a) Connolley, M. L. *J. Appl. Crystallogr.* **1983**, *16*, 548. (b) Cerius2 V3.0 Software, Molecular Simulations Inc.: San Diego, CA.

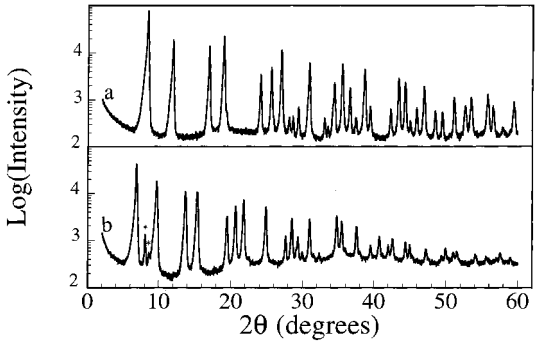

Figure 5. X-ray powder diffraction patterns of (a), **PtPt** and (b) **PtPt**·$12H_2O$. Peaks marked with * are from an intermediate hydrated phase. The vertical axis in each case is the log (intensity) to more clearly show the weak diffraction peaks.

determine the space group but they do not contribute substantially to many of the observed lines in the powder data. As a potential alternate space group, we have considered *I*4/*m*. *I*4/*m* has the same systematic extinctions as *P*4/*mnc* for the metal atom positions but the conditions differ from *P*4/*mnc* when scattering from the light atoms is included. *I*4/*m* requires layers of ions parallel to the *xy* plane identical to those in MGS, but with slight differences in the arrangement of adjacent layers. Data for the 14 powder patterns collected (in four cases data were collected for two different preparations of the same material) yield only five weak reflections that violate the *P*4/*mnc* extinctions and only nine violations of the *I*4/*m* extinctions. In both cases, most of the violations occur in weak overlapping reflections where the indexing is less than certain. The simplest explanation, and the one we favor, is that all of these compounds have the MSG structure (*P*4/*mnc*), but we cannot rule out the related *I*4/*m* structure. It may be possible to resolve this question through Rietveld refinement,[16] but more extensive data need to be collected for this to be feasible. In any event, the space group assignment is only an issue with regards to the ligand torsional angles in the structure.

Exposure of both dry **PtPt** and **PtPd** to water vapor results in a reversible expansion of the unit cell and retention of tetragonal symmetry (Figure 5). After 4 h of exposure of **PtPd** to 100% relative humidity air, a powder pattern was collected and indexed to a tetragonal unit cell with dimensions $a = 18.224(3)$ Å and $c = 6.326(1)$ Å. Similar exposure of **PtPt** also gave a tetragonal unit cell with dimensions $a = 18.271(4)$ Å and $c = 6.325(1)$ Å. Careful examination of this latter powder pattern shows small peaks in the pattern at $d = 11.0875$ and 10.3143 Å (labeled with an asterisk in Figure 5) that could not be indexed to either tetragonal cell. Fast powder diffraction scans (see the Experimental Section) showed that these peaks are the intense, low-angle reflections that belong to one or more intermediate phases that grow in and then decay as the sample is exposed to water vapor but before equilibrium is established. Similar behavior was observed for the uptake of methanol vapor by both **PtPt** and **PtPd**; results for **PtPt** are shown in Figure 6. In this case the changes in the powder diffraction pattern are simpler—a single intermediate that is tentatively assigned to a tetragonal phase with $a = 16.7$ Å. This value is between $a = 14.731(1)$ Å for **PtPt** and $a = 18.698(5)$ Å for **PtPt**·8 methanol. The observation of this intermediate phase is also in agreement with the observation of a second process in the methanol uptake gravimetric data and we tentatively assign its stoichiometry as **PtPt**·4 methanol.

(16) Harris, K. D. M.; Tremayne, M. *Chem. Mater.* **1996**, *8*, 2554.

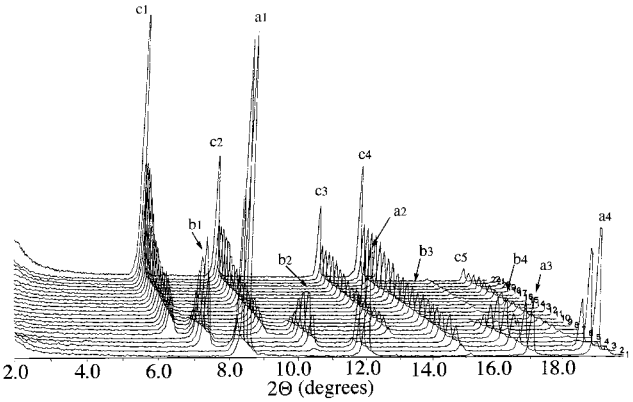

Figure 6. "Snap shot" X-ray powder diffraction patterns of **PtPt** in the presence of methanol vapor. Each repetitive scan was collected over a 6 min period from low angle to high. The horizontal axis is in degrees, the vertical axis is in intensity and the third axis (into the paper) is the number of each sequential scan. Peaks labeled **a** are attributed to dry **PtPt**; those labeled **b** are attributed to the intermediate **PtPt**·4MeOH phase; those labeled **c** are due to **PtPt**·8MeOH. Peak labels identify peaks with identical indices.

Discussion

Although the color changes associated with the vapochromism exhibited by the **PtPt** and **PtPd** complexes are not as dramatic as those of the previously studied $[Pt(p\text{-}CN\text{-}C_6H_4\text{-}C_{10}H_{21})_4]$-$[M(CN)_4]$ (M = Pt, Pd) systems,[1,3] the favorable solubility properties of the complexes in water and the formation of a variety of solid-state hydrates and solvates of sufficient microcrystallinity make this an excellent system for X-ray diffraction studies of vapochromism. Table 3 contains a summary of the unit cell data for the single-crystal study of the monoclinic hydrated phase (**PtPt**·$16H_2O$) and the various dry and hydrated/solvated tetragonal phases that we have characterized by powder diffraction studies.

A most striking result is the small variation of the stacking direction cell parameter (*b* in the monoclinic crystal, *c* in the tetragonal phases) with changes in anion metal (Pt or Pd) and hydration/solvation level. The average values of the *c*-axis length for all of the **PtPt** and **PtPd** tetragonal phases are $c = 6.3368(5)$ Å and 6.3431(5) Å, respectively; the changes observed in *c* from phase to phase are statistically significant but are small compared with those observed in other compounds containing PtL_4 stacks such as $M_xPt(CN)_4$·nH_2O.[10a] The small changes that are observed in the M−M distance associated with hydration/solvation are consistent with strong ionic interactions that hold the cations and anions together in the stacks irrespective of changes in the interchain interactions. Equally striking is the wide variation in the distance between neighboring chains in the *ab* plane. In the dry tetragonal PtPt complex, the chains are separated by 10.416(1) (cation−anion) and by 14.731(1) Å (cation−cation, anion−anion). In the corresponding tetragonal hydrate, these distances are 12.920(4) and 18.271(4) Å. The slipped nature of the stacks in the monoclinic compound complicates comparison; however, interionic distances in this case are 12.456(2) and 16.148(2) Å for cation−anion distances along *a* and *c*, respectively. Cation−cation and anion−anion distances are 14.719(2) and 14.721(2) Å, respectively. The single-crystal structure of the monoclinic hydrate clearly shows that the stacks are separated from each other by a network of hydrogen bonds between the water molecules and the cyanide ligands. The ATR FT-IR studies suggest similar interactions exist in the tetragonal hydrates with both anions. The tetragonal organic solvates exhibit even longer interchain distances of

13.221(5) Å (cation−anion) and 18.698(4) Å (cation−cation, anion−anion) for methanol, 13.648(4) and 19.330(1) Å for trifluoroethanol, and 14.540(4) and 20.563(4) Å for chloroform, respectively. In these latter cases the size of the guest is larger and the possibilities for the formation of extended hydrogen bonding networks are diminished relative to water; however, IR spectroscopy indicates that all of these organic guests are H-bonded to the cyanide ligands of the $[Pt(CN)_4]^{2-}$ anions.

Clearly the large changes in the unit cell dimensions that we observe suggest that these compounds do not behave as "organometallic zeolites" with well-defined pore sizes such as those found in β-$Ni(NCS)_2(Me\text{-}Py)_4$ host−guest compounds[17] where the unit cell volume changes are not large enough alone to accommodate the guest molecules. Apparently, the entry of the guest into the **PtM** vapochromic materials typically generates "new" space created by the large unit cell expansion. Perhaps the kinetics of the expansion is more influenced by the void space that arises from inefficient packing in the dry materials. Only in the case of trifluoroethanol does the packing efficiency decrease from the dry value and in this case the decrease is small. An analysis of the volume[15] of the dry tetragonal form of **PtPt** indicates that the atoms occupy 427 Å^3 leaving a free volume of 259 Å^3 per formula unit. This generates a packing coefficient (C_K) of 0.622 for the dry tetragonal form of **PtPt** that is extremely low compared with the C_K value of 0.887 for MGS and at the low end of the accepted range commonly observed for organic molecules. For example, the packing coefficient (C_K) for organics ranges from 0.595 for the poorly packed 2,6-di-*n*-octylnaphthalene to 0.887 in graphite.[18] Although a low value of the packing coefficient could indicate a lattice with pores of molecular size, it is more reasonable to atttibute the low C_K value in the guest free material to uniformly poor packing. In contrast to the tetragonal forms, the monoclinic hydrated phase (**PtPt**·$16H_2O$) exhibits a much higher packing coefficient of 0.716 that probably reflects the efficient packing of the water molecules enabled by the extensive H-bonding network.

The packing coefficients were also calculated (Table 3) for the tetragonal unit cells that contain solvent (12 water, 8 methanol, 6 chloroform, and 4 trifluoroethanol per formula unit). For these solvents the unit cell volume expansions are remarkably large and increase in the following order: dry < H_2O (54%) < methanol (60%) < CF_3CH_2OH (73%) < $CHCl_3$ (94%) (where the values in parentheses are the percent volume increases relative to the dry). The molecular volumes for these guests follow the same trend: H_2O (22.3 Å^3) < methanol (36.6 Å^3) < CF_3CH_2OH (70.5 Å^3) < $CHCl_3$ (74.8 Å^3), even though the stoichiometry of each compound is different. Tentatively, these measurements suggest that the magnitude of the lattice expansion is influenced by the size of the guest vapor and the number of guests rather than by the size of preexisting pores in the host. This type of lattice expansion suggests that if the guest−host interactions are favorable, even large molecules could enter the lattice. Further work designed to realize this situation is in progress.

Finally, we propose a schematic mechanism (outlined specifically for methanol) in Figure 7 for the unit cell expansion that we observe when **PtPt** or **PtPd** sorb water or organic solvents. The guest molecules enter the lattice and separate the chains

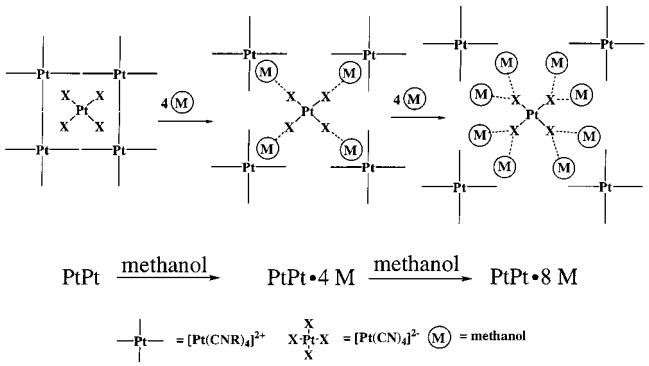

Figure 7. A schematized view down the tetragonal *c*-axis that illustrates the proposed mechanism of crystalline **PtPt** sorbing methanol vapor. One layer in the ab plane is shown at three stages of methanol sorption. The next layer up (a, b, $^1/_2$) is slipped so that a cation is above each anion etc.

but preserve the tetragonal symmetry and the spacing along the *c*-axis. Important hydrogen bonding interactions occur between the cyanide ion nitrogen and the guest; additional H-bonding is also expected when it is feasible (i.e., water). In the case of water, the H-bonding interactions are so favorable that the continued sorption of water leads to the formation of multiple hydrates and finally to dissolution of the compound.

Conclusions

Powder diffraction studies show that anhydrous **PtPt** and **PtPd** adopt tetragonal space groups with nearly identical lattice constants. The structures of these materials and the tetragonal hydrate/solvates that we have characterized are probably analogues of the well-known Magnus' green salt (space group *P*4/*mnc*) with alternating cations and anions along the *c*-axis. The tetragonal plane unit cell lengths expand dramatically and reversibly when guests are sorbed. Significant H-bonding interactions are present between the guest molecules and the cyanide ligands of the tetracyanometalate anions. The data are consistent with small changes along the *c* axis and consequently small changes in the **ground state** M−M distance when solvent molecule guests are sorbed by this system. More importantly, there is not a significant correlation (such as the relationship of Gliemann[10a] that relates the energy of the low-energy band in $M_x[Pt(CN)_4]\cdot nH_2O$ compounds to $1/R^3$ (where R is the M−M distance)) between the M−M distance and the observed vapochromic shifts. These results, in combination with our other recent work,[3] suggest that H-bonding (where energetically feasible) or lypophilic interactions in the plane perpendicular to the chain axis are more important factors that influence the magnitude of the vapochromic shift of the "M−M charge transfer" transition in the systems studied here.[10a] Exactly how these interactions produce the vapochromic shift is not known; perhaps they affect the excited-state M−M distance or coupling by changing the polarity of the medium surrounding the chromophore. Additionally, it is an open question whether the vapochromic shifts we observe for the other platinum systems we have investigated result from a similar mechanism or whether they arise from changes in the metal−metal distances. Studies of additional systems are in progress to answer these remaining questions of interest.

Acknowledgment. This work has been funded by the Center for Process Analytical Chemistry and the INEEL University Research Consortium. The INEEL is managed by Lockheed Martin Idaho Technologies Co. for the U.S. Department of

(17) For a relevant discussion of the $Ni(SCN)_2L_4$ inclusion systems see: *Inclusion Compounds*; Atwood, J. L., Davies, J. E. D., MacNicol, D. D., Eds.; Academic Press: New York, 1984; Vol. 1, pp 59−133.

(18) (a) Kitaigorodskii, A. I. *Organic Chemical Crystallography*; Consultants Bureau Enterprises, Inc.: New York, 1961; p 107. (b) Gavezzotti, A. *J. Am. Chem. Soc.* **1989**, *111*, 1835.

Energy, Idaho Operations Office, under contract No. DE-AC07-94ID13223. The FT-IR spectrometer was purchased with funds from NSF Grant No. CHE-9307837.

Supporting Information Available: Full details of the X-ray crystal structures of $[Pt(CN\text{-}iso\text{-}C_3H_7)_4][Pt(CN)_4]\cdot 16H_2O$ including tables listing atomic coordinates, isotropic and anisotropic displacement parameters, torsion angles, hydrogen coordinates and isotropic displacement parameters, least-squares planes, selected angles and powder diffraction patern and table for $[Pt(CN\text{-}iso\text{-}C_3H_7)_4][Pt(CN)_4]\cdot 16H_2O$ and tables of indexed X-ray powder diffraction lines for **PtPt**, **PtPt**·$12H_2O$, **PtPt**·8MeOH, **PtPt**·$4CF_3CH_2OH$, **PtPt**·$6CHCl_3$, **PtPd**, **PtPd**·$12H_2O$, **PtPd**·8MeOH, **PtPd**·$4CF_3CH_2OH$, **PtPd**·$6CHCl_3$ (30 pages, print/PDF). See any current masthead page for ordering information and Web access instructions.

JA981218C